

Article

Mechanism and Application of Roof Cutting by Directional Energy-Cumulative Blasting along Gob-Side Entry

Eryu Wang *, Zhen Shi *, Wenyuan Xi, Jiwei Feng and Pengfei Wu

School of Mining and Coal Engineering, Inner Mongolia University of Science and Technology, Inner Mongolia, Baotou 014010, China

* Correspondence: 2019958@imust.edu.cn (E.W.); sz13214916107@163.com (Z.S.); Tel.: +86-130-3958-6452 (E.W.)

Abstract: In this paper, roof-cutting technology of directional energy-cumulative presplitting blasting is taken as the research object. Through the numerical simulation software Ansys/Ls-dyna3D, the process of energy-cumulative blasting and non-cumulative blasting is simulated and analyzed by using the ALE algorithm. Moreover, the evolution processes of tensile strain energy, detonation stress wave of explosives, stress state of rock mass, and rock crack damage cumulative are compared in two conditions. In the energy cumulative state, the detonation wave acts centrally on the hole wall in the energy cumulative direction to form an initial crack, and then under the action of the jet of energy cumulative, the crack continues to propagate until it runs through. In the non-energy cumulative state, the crack propagates uniformly around the hole wall, forming irregular short cracks. The simulation is verified by the field test, and the law of crack propagation is the same with the simulation. Therefore, directional energy-concentrated presplitting blasting has good practicability in a roof presplitting operation.



Citation: Wang, E.; Shi, Z.; Xi, W.; Feng, J.; Wu, P. Mechanism and Application of Roof Cutting by Directional Energy-Cumulative Blasting along Gob-Side Entry. *Sustainability* **2022**, *14*, 13381. <https://doi.org/10.3390/su142013381>

Academic Editors: Baoqing Li, Jing Li, Jijun Tian and Beilei Sun

Received: 12 September 2022

Accepted: 12 October 2022

Published: 17 October 2022

Publisher's Note: MDPI stays neutral with regard to jurisdictional claims in published maps and institutional affiliations.



Copyright: © 2022 by the authors. Licensee MDPI, Basel, Switzerland. This article is an open access article distributed under the terms and conditions of the Creative Commons Attribution (CC BY) license (<https://creativecommons.org/licenses/by/4.0/>).

Keywords: roof structure; directional concentrated blasting; roof cutting; ALE algorithm; numerical simulation

1. Introduction

In today's world energy system, coal is still the main supply of energy in the world, including in China. Roadway is the lifeblood of China's coal mining industry; roadway roof structure stability plays an important role in the coal mining industry. The roadway support system has been strengthened and optimized to prevent roadway deformation, but relying solely on the support system is not a long-term strategy. The crack structure of hard roofs and high stress concentrations are the two main factors leading to roadway failure [1–3]. When the roadway is subjected to the coupling of dynamic and static loads, it may become unstable. The phenomenon of high stress concentration under static load and the movement of the fracture structure under dynamic load will have an impact on the surrounding rock of the roadway [4]. Based on my pressure effect and rock swelling characteristics, He [5] put forward the technology of bi-directional concentrated energy tensile blasting to control the structural stability of the roadway roof. With this technology, the roadway roof is presplit by using concentrated energy presplitting blasting, after which the roof collapses and expands along the presplitting surface and fills the goaf, effectively supporting the high roof to improve the surrounding rock stress environment and reduce the occurrence probability of rock burst accidents. Blasting technology is widely used in coal mines, tunnels, and other industries in China because of its simple process and high economic benefits [6]. Aiming at the roof cutting cumulative presplitting blasting of roadway along goaf, experts and scholars around the globe have conducted a significant amount of research. Based on the cracking mechanism of coal and gangue in multi-directional concentrated blasting, Pan [7] and others analyzed the propagation law of the blasting stress wave. Through similar simulation experiments, it is proved that multi-directional concentrated blasting is scientific and feasible. Ren [8] studied

the roof-cutting parameters, roadway support parameters, and stress and deformation law of roadway-surrounding rock under complex thin coal seam by means of numerical simulation, theory, and field experiments. Guo [9] and others carried out the study of roof cutting by concentrated blasting according to the characteristics of shallow and deep coal seam, and determined the key parameters, such as cutting angle, height, and hole spacing. Zong and Meng [10] analyzed the propagation law of the explosive detonation wave and the energy transfer characteristics under different charge structures. Liang [11], according to the propagation mechanism and fracture mechanism of the detonation stress wave in a bi-directional concentrated tension blasting, established a numerical model to study the damage degree of blasthole surrounding rock, the law of detonation stress wave energy propagation, and crack propagation under energy cumulative and non-energy cumulative conditions. Guo [12], based on the dynamic action theory of concentrated blasting, the energy cumulative mechanism, and the forming mechanism of shaped jet, analyzed the characteristics of crack expansion in coal seam blasting, established the numerical model, and analyzed the formation and migration process of shaped jet. Yang [13] et al. used the dynamic caustics test system to analyze the dynamic process and characteristics of crack propagation under the action of a single blasthole, and explored the law of crack propagation in the direction of connection between the empty hole and the blasthole under the action of blasting. Esen et al. [14] proposed a new engineering model to predict the degree of fragmentation around the blasting hole. Based on the crack-forming mechanism of bi-directional energy-cumulative blasting, Shi et al. [15] calculated the crack length of the stress wave, established the numerical model of energy-cumulative blasting, and analyzed the crack propagation length of rock under the action of blasting. Wu and others [16] established the mechanical model of concentrated blasting based on the mechanism of concentrated blasting, and analyzed the mechanism of initial crack formation in the state of concentrated energy.

Therefore, in order to improve the stability of the roadway roof and reduce the probability of accidents in the roadway, research on the roof cutting technology of concentrated blasting is of great significance. Through the methods of theoretical analysis, numerical simulation, and field test, this paper takes the 6302 working face of the Baoshan Coal Mine of Yitai Group in Inner Mongolia as the background. The north side of the Baoshan Coal Mine is the 6303 working face, while the southeast of the Baoshan Coal Mine is the 6301 working face. The length of the working face is 200 m, the thickness of the coal seam is 1.5~1.6 m, the buried depth is 53.5 m~73.7 m, the dip angle of coal seam is 1~3°, and the roof lithology includes mudstone, sandy mudstone, and medium-grained sandstone. The direct bottom and the old bottom are sandy mudstone and medium-grained sandstone, respectively.

2. Fracture Principle of Rock Mass by Concentrated Blasting

2.1. Mechanism of Bi-Directional Energy-Concentrated Tensile Blasting

Bi-directional concentrated tensile blasting mainly makes use of the characteristics of high compressive strength and low tensile strength of rock. This technology can change the dynamic process of interaction between detonation wave and surrounding rock after explosive explosion. Detonation wave acts on the surrounding rock of blasthole, uniformly compressed in the non-energy cumulative direction and concentrated tension in energy cumulative direction [5]. The explosive gas pressure is converted to the tension in the energy cumulative direction to the maximum extent, so as to produce an effective slit surface and achieve the purpose of cutting the top. The mechanism is shown in Figure 1.

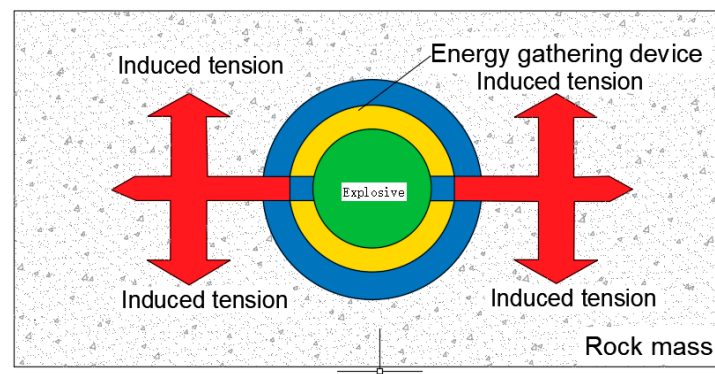


Figure 1. Mechanism of biaxial concentrated tensile blasting.

After the explosion, under the action of the energy cumulative device, the detonation wave is first unloaded from the set direction and acts directly on the surrounding rock of the blasthole along the set direction, resulting in an initial crack on the surrounding rock of the blasthole. Under the guidance of energy, the high-pressure, high-temperature, and high-speed impact gas [17,18] produced by detonation still flows into the initial crack along the set direction and forms a “gas wedge”, which causes the crack to continue to expand until the explosive in the blasthole is exhausted. In the non-set direction, because the energy cumulative device itself has a certain strength and thickness, it will reduce the propagation of the stress wave in the non-set direction to a certain extent and restrain the detonation wave, and because of the energy cumulative device and the annular space with the blast hole wall, it will also reduce the direct action and damage of detonation gas on the hole wall, resulting in rock mass tensions that are cracked along the set direction, resulting in the formation of slits. The surrounding rock with a non-set direction still maintains good integrity relative to the jet direction.

2.2. Mechanism of Crack Initiation and Propagation

In the non-energy cumulative state, the detonation products will disperse irregularly inside the blasthole, so the rock mass around the blasthole is seriously damaged, and the cracks are irregularly divergent [19]. After the detonation of the explosive, the detonation air flow generated first gathers in the set direction and acts directly on the hole wall rock along the energy concentrator. In the early stage of blasting, the borehole wall is mainly affected by the explosion stress wave, and in a later stage, it is mainly affected by the static pressure of explosive gas. The shaped charge jet on the surrounding rock of the blasthole produced a certain range of failure zone and crack development zone under the action of the explosion stress wave, that is, the initial oriented slit, and the explosive gas also entered the initial crack and promoted the further expansion of the crack.

According to the theory of fracture mechanics, $\partial\sigma_\theta/\partial\theta = 0$, $\partial^2\sigma_\theta/\partial\theta^2 < 0$, and $K_H = 0$, then by the formula:

$$\left(\begin{array}{l} \sigma_\gamma = \frac{1}{2(2\pi\gamma)^{1/2}} [K_1(3 - \cos\theta) \cos\frac{\theta}{2} + K_H(3\cos\theta - 1) \sin\frac{\theta}{2}] \\ \sigma_\theta = \frac{1}{(2\pi\gamma)^{1/2}} \cos\frac{\theta}{2} [K_1 \cos^2\frac{\theta}{2} - \frac{3}{2}K_H \sin\theta] \\ \sigma_{\gamma\theta} = \frac{1}{2(2\pi\gamma)^{1/2}} \cos\frac{\theta}{2} [K_1 \sin\theta + K_H(3\cos\theta - 1)] \end{array} \right) \quad (1)$$

The propagation angle of the crack can be obtained:

$$\theta_0 = 0$$

Therefore, it can be obtained that under the action of static pressure, the new cracks in the surrounding rock will continue to expand in accordance with the original cracks,

resulting in a large range of extended radial cracks in the set direction of the energy concentrator, forming top-cutting cracks.

The stress intensity factor at the tip of crack propagation [20] is:

$$K = PF\sqrt{\pi(r + \alpha)} + \sigma\sqrt{\pi\alpha} \quad (2)$$

where P is the pressure of explosive gas; F is the correction coefficient of the stress intensity factor at the crack tip; r is the radius of the hole; α is the instantaneous length of crack propagation; σ is tangential stress.

At the end of the concentrated energy flow penetration, the stress intensity factor at the crack tip can be expressed as:

$$K_1 = P_0F\sqrt{\pi(r + \alpha_0)} + \sigma\sqrt{\pi\alpha_0} \quad (3)$$

where P_0 the pressure when the explosive gas fills the hole at the end of the penetration; F is the correction coefficient of the stress intensity factor at the crack tip; r is the radius of the hole; α_0 is the length of the crack; σ is tangential stress.

According to the theory of rock mechanics, when the fracture toughness of rock is less than the stress intensity factor at the crack tip, the rock is destroyed, which leads to crack propagation [21]. Therefore, initiation conditions of cracks are obtained as follows:

$$P_0 > \frac{K_{IC} - \sigma\sqrt{\pi\alpha_0}}{F\sqrt{\pi(r + \alpha_0)}} \quad (4)$$

where K_{IC} is the fracture toughness of rock; P_0 the pressure when the explosive gas fills the hole at the end of the penetration; σ is tangential stress; F is the correction coefficient of the stress intensity factor at the crack tip; α_0 is the length of the crack; r is the radius of the hole.

Under the action of the static pressure of the later explosive gas, the crack expands further, and with the expansion of the crack, the pressure of the explosive gas decreases continuously. In order to ensure the continuous expansion of the crack, the instantaneous pressure of the explosive gas needs to meet the following formula:

$$P > \frac{K_{IC} - \sigma\sqrt{\pi\alpha_0}}{F\sqrt{\pi(r + \alpha)}} \quad (5)$$

where K_{IC} is the fracture toughness of rock; P is the pressure of explosive gas; σ is tangential stress; F is the correction coefficient of the stress intensity factor at the crack tip; α_0 is the length of the crack; r is the radius of the hole; α is the instantaneous length of crack propagation.

In the process of crack expansion in the non-energy-concentrated state, because there is no concentrated energy flow penetration, the stress intensity factor at the crack end is:

$$K = PF\sqrt{\pi(r + \alpha)} \quad (6)$$

where P is the instantaneous pressure of explosive gas; F is the correction coefficient of the stress intensity factor; r is the radius of blasthole; α is the instantaneous length of crack propagation.

Similarly, the initiation conditions of cracks in the non-energy-accumulating direction are as follows:

$$P_0 > \frac{K_{IC}}{F\sqrt{\pi(r + \alpha_0)}} \quad (7)$$

where K_{IC} is the fracture toughness of rock; P_0 the pressure when the explosive gas fills the hole at the end of the penetration; F is the correction coefficient of the stress intensity factor; r is the radius of blasthole; α_0 is the length of the crack.

The conditions for continuous expansion of cracks in the non-energy-gathering direction are as follows:

$$P > \frac{K_{IC}}{F\sqrt{\pi(r+\alpha)}} \quad (8)$$

where K_{IC} is the fracture toughness of rock; P is the instantaneous pressure of explosive gas; F is the correction coefficient of the stress intensity factor; r is the radius of blasthole; α is the instantaneous length of crack propagation.

From the above formula, it can be seen that the penetration of concentrated energy flow in the energy cumulative direction reduces the pressure needed for crack initiation and expansion, and promotes the crack propagation distance to be larger. The results show that compared with non-concentrated blasting, concentrated blasting has the advantage of cracking and can improve the roof cutting effect.

3. Arbitrary Lagrangian-Eulerian (ALE) Algorithm

The arbitrary Lagrangian-Eulerian algorithm was first proposed by Noh (1964) as the coupled Euler-Lagrange algorithm. In this algorithm, the grid can move in any form in space, so that the moving interface of the object can be accurately described and the reasonable shape of the unit can be maintained by specifying a reasonable form of grid motion. The pure Lagrangian algorithm and the Eulerian algorithm are in fact two special cases of the ALE algorithm, that is, it is reduced to the Lagrangian algorithm when the velocity of the grid point is equal to the velocity of the material point, and to the Eulerian algorithm when the grid is fixed in space. The characteristic of the ALE algorithm is that the grid it uses is neither the fixed grid of the Eulerian algorithm nor the body grid of the Lagrangian algorithm, but constructs a set of appropriate grids according to the flow boundary of the material region.

The body derivative described by ALE can be written as follows:

$$\left. \frac{\partial F}{\partial t} \right|_X = \left. \frac{\partial F(\xi, t)}{\partial t} \right|_{\xi} + c_i \frac{\partial F}{\partial \chi_i} \quad (9)$$

where $c_i = u_i - \omega_i$ is the convective velocity described by ALE; u_i is the physical velocity of particle X ; ω_i is the grid speed.

Through Formula (9), the governing equation in the current configuration of ALE algorithm can be obtained [22]:

The mass conservation equation:

$$\left. \frac{\partial \rho}{\partial t} \right|_{\varepsilon} + c_i \frac{\partial \rho}{\partial \chi_i} + \rho \frac{\partial v_i}{\partial \chi_i} = 0 \quad (10)$$

The momentum conservation equation:

$$\rho \left. \frac{\partial v_i}{\partial t} \right|_{\varepsilon} + \rho c_i \frac{\partial v_i}{\partial \chi_j} = \frac{\partial \sigma_{ij}}{\partial \chi_j} + \rho f_i \quad (11)$$

The energy conservation equation:

$$\rho \left. \frac{\partial e}{\partial t} \right|_{\varepsilon} + \rho c_i \frac{\partial e}{\partial \chi_i} = \sigma_{ij} \frac{\partial v_i}{\partial \chi_j} - \frac{\partial q_i}{\partial \chi_i} \quad (12)$$

where ρ represents density; f_i represents physical strength per unit mass; χ represents the coordinates of matter in the grid; v represents the speed of motion; t represents time; c represents the convection velocity; ε represents the position vector in the reference

coordinates; σ_{ij} represents the Cauchy stress tensor; e represents internal energy per unit mass; q_i represents the heat flux.

4. Numerical Simulation Research

4.1. Numerical Modeling and Meshing

In the field construction, the roof cutting by concentrated blasting usually adopts the structure of continuous charge. In order to facilitate the calculation, the blasthole and rock mass profiles are obtained for analysis. The nonlinear dynamic software is used to simulate the two-way concentrated blasting, the Ansys software is used for modeling, and the SOLID164 element in the software is used to establish the model. The model is divided into four parts: rock, air, explosive, and energy concentrator. In the model, the area of air and rock mass is $100\text{ cm} \times 100\text{ cm}$ square, the inner diameter of the concentrating tube is 3.6 cm , the outer diameter is 4.2 cm , the slit width is 0.4 cm , and the diameter of the explosive is 3.2 cm . The calculation model is simplified to the plane stress state, and 1 cm is taken as the thickness direction. After the establishment of the model, the meshing is divided by mapping and sweeping, while the local mesh refinement is beneficial to the transmission pressure, so the air and rock grids near the explosive area are refined, and the energy concentrator and explosive are divided into uniform grids, as shown in Figure 2. Because the rock and air elements will produce a large deformation in the blasting process, and the mesh distortion caused by large deformation may affect the calculation results, the ALE algorithm is used here. The Lagrange element is used for the rock and energy tube, the ALE element is used for explosive and air, and the coupling of structure and air is realized by the keyword *CONSTRAINED_LAGRANGE_IN_SOLID. In the calculation process, the explosive is initiated by the central point, while the boundary conditions of air and rock are non-reflective. In order to obtain the energy cumulative effect of energy cumulative blasting, a model with the same size and the same parameters except the energy cumulative tube is established, while the energy cumulative and non-energy cumulative stress evolution laws are analyzed and compared, and the energy cumulative effect of energy cumulative blasting is obtained.

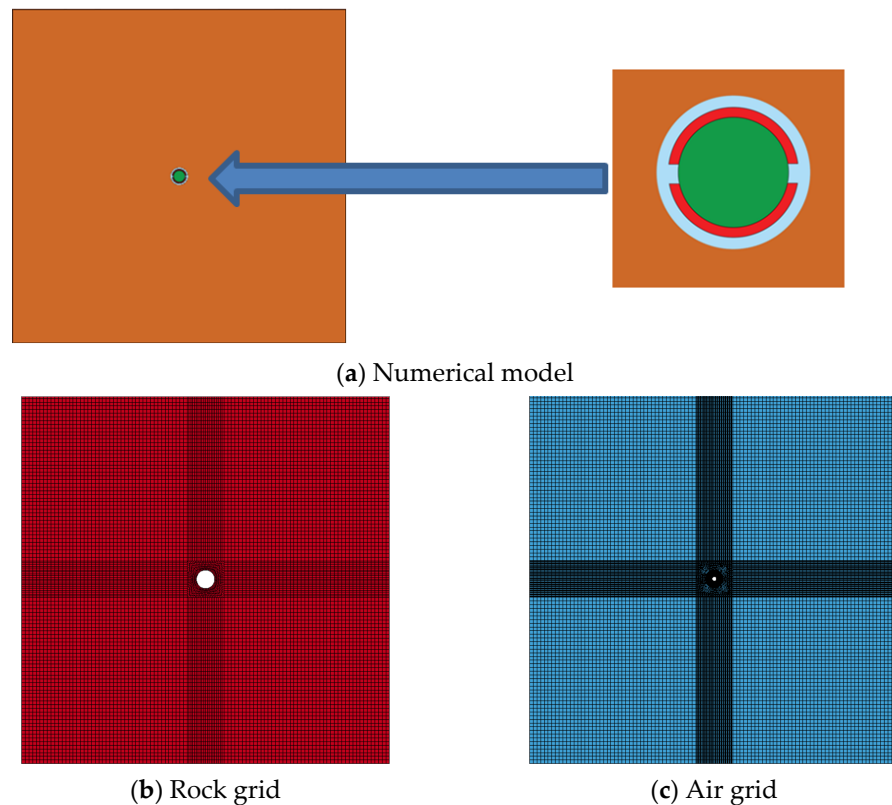


Figure 2. Cont.

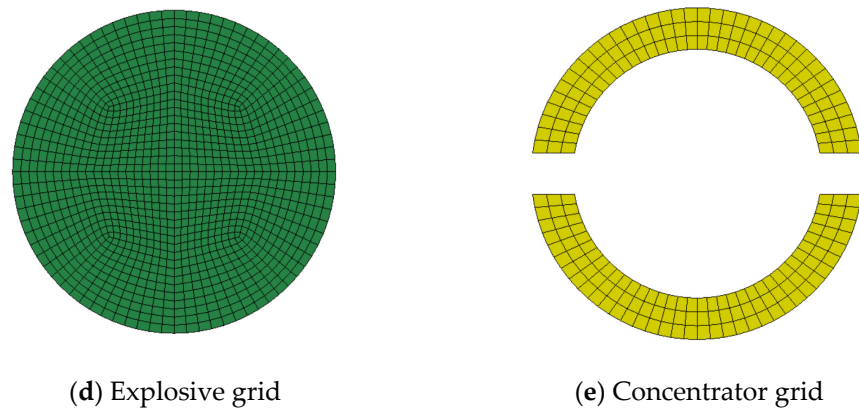


Figure 2. Numerical simulation model diagram and meshing.

4.2. Determination of Model Calculation Parameters

4.2.1. Explosive Parameters

The explosive adopts two-stage emulsion explosive, the explosive material model adopts the *MAT_HIGH_EXPLOSIVE_BURN model, and the detonation pressure is expressed by the JWL equation of state [23]:

$$p = A \left(1 - \frac{\omega}{AR_1} \right) e^{-R_1 V} + B \left(1 - \frac{\omega}{AR_2} \right) e^{-R_2 V} + \frac{\omega E}{V} \quad (13)$$

where p is the pressure of detonation products; A , B , R_1 , and R_2 are material constants; V is the relative volume of detonation products; E is the initial internal energy density of the detonation products.

The explosive parameters are shown in Table 1.

Table 1. Mechanical parameters of explosives.

RO/ (g·m ⁻³)	D/ (m·μs ⁻¹)	PCJ/ Mbr	JWL Equation of State				
			A/ Mbr	B/ Mbr	R ₁	R ₂	ω
1.18	0.5122	0.0953	2.762	0.0844	5.2	2.1	0.5

4.2.2. Material Parameters of Energy Concentrator

PVC material is used in the energy concentrating tube in the project site, this kind of material is a heat-related material, which has a certain strength in the initial stage of blasting reaction, but under the impact of detonation products and high temperature, it will be destroyed [24,25], so it is simulated by the *MAT_PLASTIC_KINEMATIC plastic constitutive model. The *MAT_ADD_EROSION keyword is used to set a small restart, and a part of the energy concentrator is deleted after the failure of the energy concentrator to prevent the failure of the energy concentrator from affecting the simulation results.

The material parameters of the concentrator are shown in Table 2.

Table 2. Mechanical parameters of concentrating tube materials.

RO/(g·cm ⁻³)	PR	E/ Mbr	SIGY/ Mbr	ETAN/ Mbr
8.93	0.35	1.17	0.004	0.001

4.2.3. Air Material Parameters

Because the energy concentrating tube does not fully fit the hole wall, the air domain should be set. Air is regarded as an ideal gas. The equation of the air material selection* MAT_NULL model is described by * EOS_LINEAR_POLYNOMIAL:

$$P = C_0 + C_1\mu + C_2\mu^2 + C_3\mu^3 + (C_4 + C_5\mu + C_6\mu^2)E \quad (14)$$

where $C_0, C_1, C_2, C_3, C_4, C_5, C_6$ are constant; μ is the specific volume; E is the specific internal energy.

The air material parameters are shown in Table 3.

Table 3. Mechanical parameters of air materials.

RO/(g·cm ⁻³)	* EOS_LINEAR_POLYNOMIAL							E ₀
	C ₀	C ₁	C ₂	C ₃	C ₄	C ₅	C ₆	
1.2	0	0	0	0	0.4	0.4	0	2.5 × 10 ⁻⁶

4.2.4. Rock Material Parameters

In the process of explosion, the rock mass is damaged in two forms: one is tensile failure and the other is compression failure. Furthermore, the rock around the blasthole is in a state of large strain, high strain rate, and high stress during blasting; according to this characteristic, the rock adopts * MAT_JOHNSON_HOLMQUIST_CONCRETE, that is, the HJC model. Since rock cracking and crack propagation are realized by rock failure, the keyword * MAT_ADD_EROSION is used to add tensile stress and shear strain damage failure criteria to simulate the dynamic failure effect of rock [26].

The rock material parameters are shown in Table 4.

Table 4. Mechanical parameters of rock materials.

RO/(g·cm ⁻³)	G/Mbr	A	B	C	N	FC/Mbr	T/Mbr	EPS0/μs ⁻¹	E _{fmin}	S _{fmax}
2.6	0.287	0.28	2.5	0.00186	0.79	0.00154	1.708 × 10 ⁻⁴	1.0 × 10 ⁻¹¹	0.01	5.0
P _c /Mbr	μ _c	P ₁ /Mbr	μ ₁	D ₁	D ₂	K ₁ /Mbr	K ₂ /Mbr	K ₃ /Mbr	F _s	
1.0 × 10 ⁻⁴	0.00162	0.012	0.012	0.04	1.0	0.12	0.25	0.42	0.035	

4.3. Comparison and Analysis

The crack propagation process is shown in Figures 3 and 4.

In order to obtain the change law of mechanical properties of concentrated blasting and non-concentrated blasting during blasting, measuring points A, B, C, D, and E were arranged at 5 cm, 15 cm, 25 cm, 35 cm, and 45 cm, respectively, to monitor the changes of mechanical properties of each point during blasting. The location of the measuring point is shown in Figure 5.

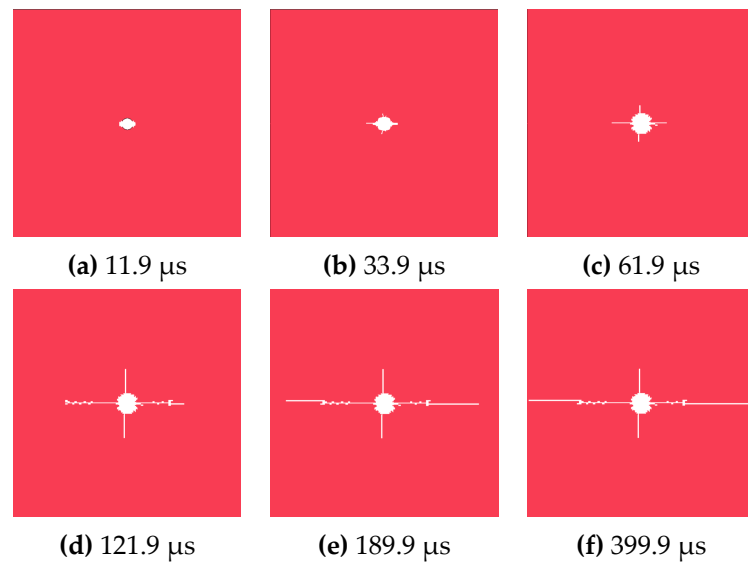


Figure 3. Crack propagation process of rock under the energy cumulative condition.

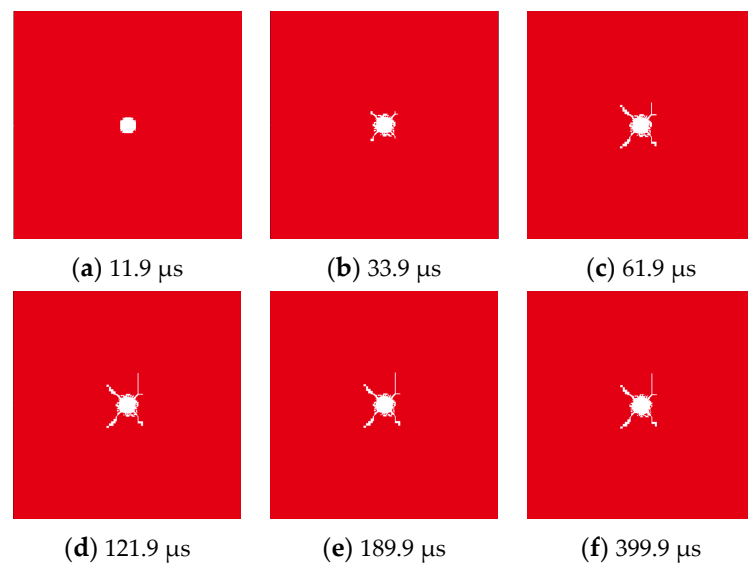


Figure 4. Crack propagation process of rock under the non-energy cumulative condition.



Figure 5. Arrangement of blasting monitoring points.

4.3.1. Energy Evolution Process

It can be seen from Figure 6 that under the action of the energy accumulator, the energy produced by the explosive explosion in the state of 11.9 μs produces a jet in the energy cumulative direction, and the energy in the energy cumulative direction is enhanced and

weakened in other directions. The energy wave propagates outward in a fan shape along the energy cumulative direction. At $33.9 \mu\text{s}$, the energy first acts on the hole wall from the set direction to form a guiding initial crack, then the energy propagates outward along the direction of the initial guiding crack, and a high stress zone is formed at the crack tip. Because the stress in the high stress area is greater than the fracture toughness of the rock, the crack deepens continuously in the range of $33.9 \mu\text{s}$ to $399.9 \mu\text{s}$. As can be seen from Figure 7, under the non-energy cumulative condition, the explosion stress wave propagates gradually and uniformly along the blasting hole, and the blasting energy acts uniformly on the wall of the blast hole. At $11.9 \mu\text{s}$, the detonation wave acts on the surrounding rock of the blast hole, and the failure area is approximately circular. The crack expands continuously between $33.9 \mu\text{s}$ and $121.9 \mu\text{s}$. At $189.9 \mu\text{s}$, because the stress in the high stress area at the crack tip is lower than the fracture toughness of the rock, the crack stops expanding and the surrounding stress tends to be stable. Under the action of the energy cumulative device, the length of the rock crack in the energy cumulative state is much longer than that in the non-energy cumulative state. It can be seen from Figure 8 that the energy of the detonation wave in two states decreases with the increase of propagation distance, and the energy of each measuring point in the energy cumulative direction is much larger than that of each measuring point in the non-energy cumulative state, i.e., 2.3 times, increasing the action time. The utilization rate of explosive energy is improved.

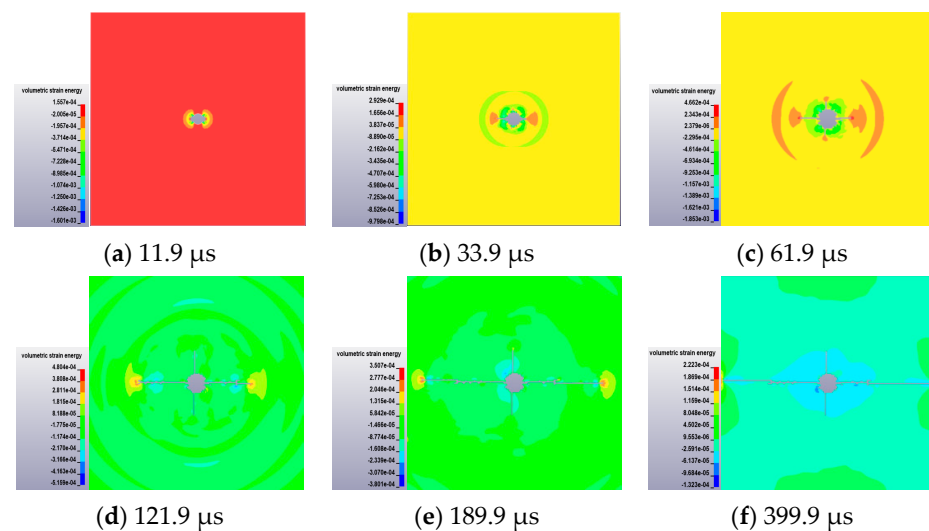


Figure 6. Energy change process of energy cumulative blasting.

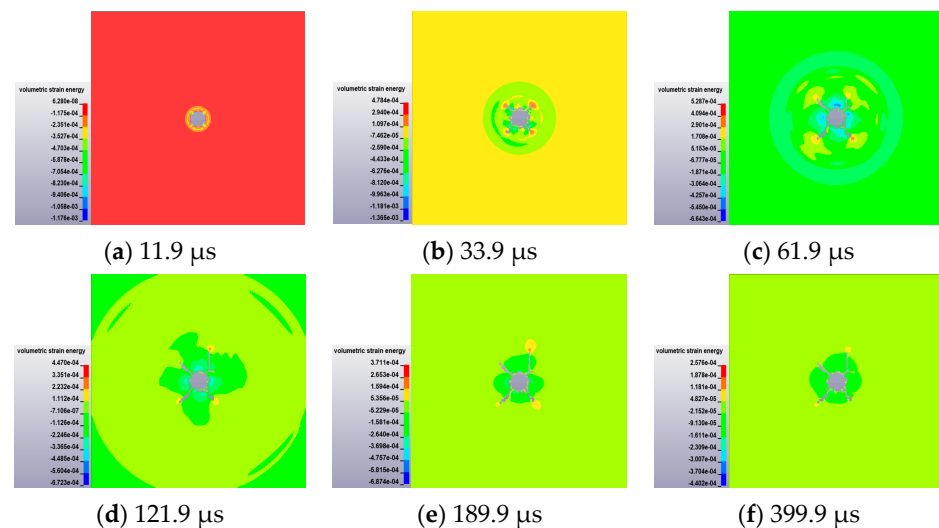


Figure 7. Variation process of non-energy cumulative blasting.

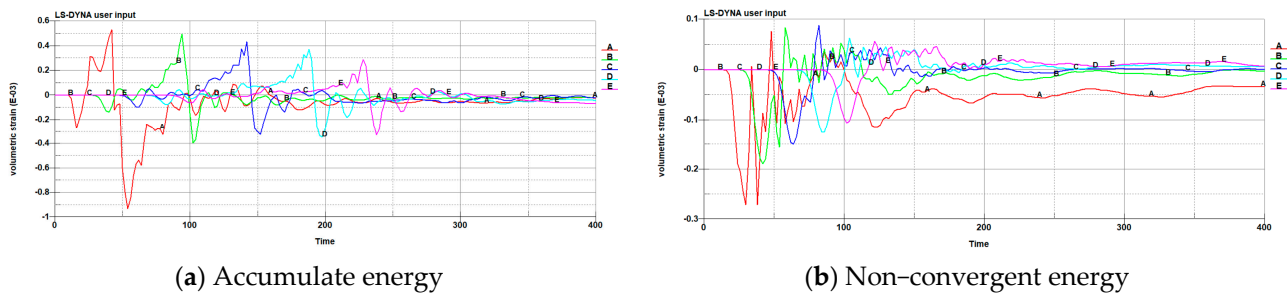


Figure 8. Energy time history curve.

4.3.2. Detonation Stress and Velocity Propagation Process

From the combination curve of the detonation wave stress and velocity cloud diagram (Figures 9–14), it can be seen that in the energy cumulative direction, the explosive propagates preferentially to the energy cumulative direction, forms a high stress zone and a high velocity zone in the energy cumulative direction, and becomes stronger with time. After the detonation wave propagates to the wall of the blasthole along the energy cumulative direction, the stress strength of the detonation wave is greater than the dynamic tensile strength of the rock mass, and a guide crack is formed under the action of the jet. Since then, under the influence of the propagation characteristics of the detonation wave, the detonation wave continues to propagate along the energy cumulative direction. At 61.9 μs , the energy cumulative tube is greatly damaged by high stress deformation, and the detonation wave also has an effect on the hole wall in the non-energy cumulative direction. At this time, the hole wall is destroyed. Part of the detonation wave will continue to reflect in the process of propagation, and the new stress wave will continue to act on the tip of the notch, making the fracture continue to develop. In the process from 61.9 μs to 399.9 μs , with the penetration of a detonation wave, the crack deepens until it penetrates. In the non-energy cumulative direction, under the influence of the energy cumulative device, the detonation energy transferred to the borehole wall is weakened and the failure area is reduced. In the non-energy-gathering state, the detonation wave propagates outward in a ring, acting uniformly on the hole wall, and the hole wall is uniformly forced to form a near-circular failure area. The detonation wave stress and velocity around the blasthole propagate uniformly and gradually decrease with the propagation distance until the end of the blasting process. There are differences in the arrival time and magnitude of the peak at each measuring point under energy cumulative and non-energy cumulative conditions. The velocity transfer of detonation wave in the non-concentrated state lags about 20 μs compared with that in the concentrated state, and the peak value of each measuring point in the concentrated state is about 2.2 times of that in the non-concentrated state, and the propagation speed is fast. The peak value of stress and velocity of detonation wave at measuring point An is the largest, and the peak value decreases gradually with the distance from the hole wall, but under the action of concentrated jet, the attenuation velocity of peak stress and velocity of detonation wave under the condition of concentrated energy is smaller than that under the action of non-concentrated energy. The peak stress of detonation wave at each measuring point in the energy cumulative state is larger than that in the non-energy cumulative state, so the peak stress of rock mass in the energy cumulative direction is larger under the action of energy cumulative device during blasting, which promotes the development and expansion of cracks. In addition, due to the action of a jet, the attenuation velocity of detonation wave stress in rock mass in the energy cumulative direction is the smallest, which expands the range of detonation wave stress and effectively improves the utilization rate of explosive energy.

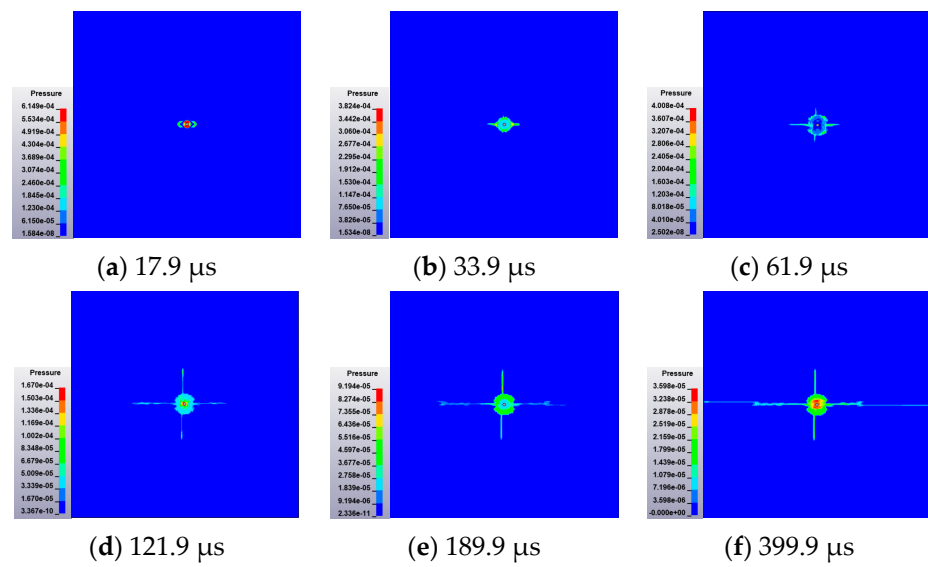


Figure 9. Evolution of the detonation stress wave under the energy cumulative condition.

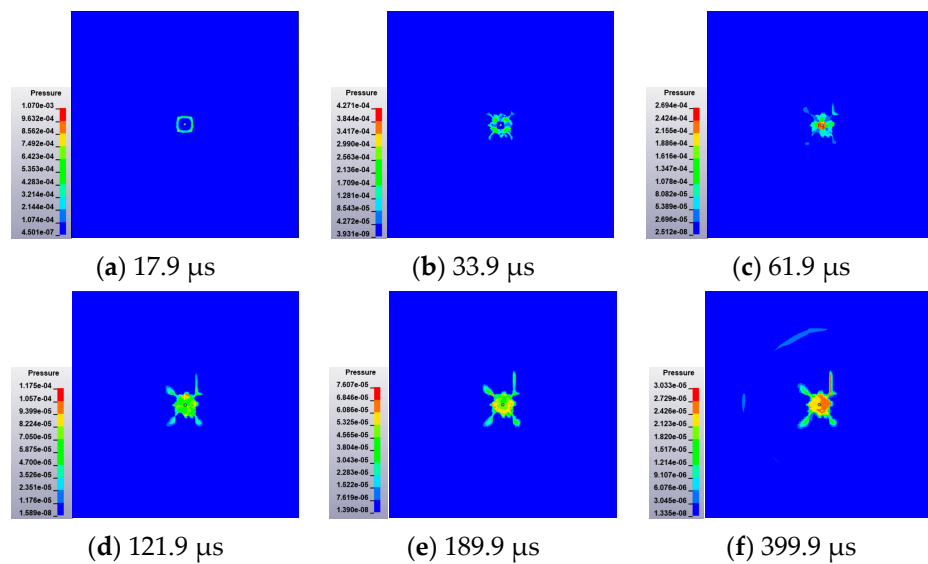


Figure 10. Evolution of detonation stress wave under the non-energy cumulative condition.

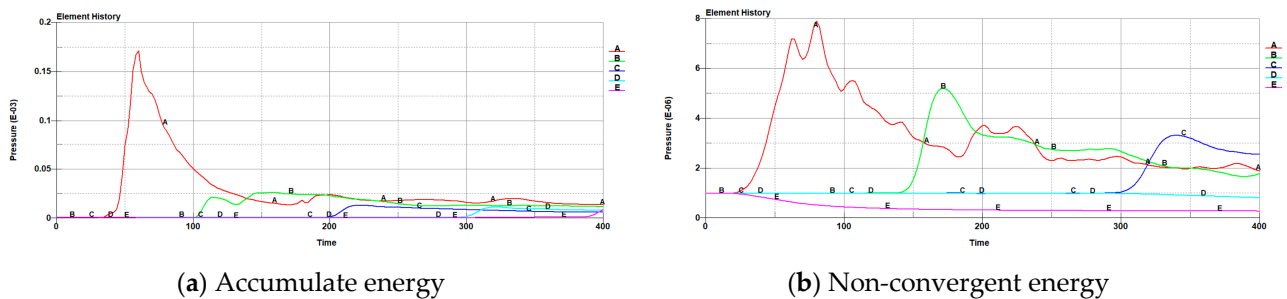


Figure 11. Detonation stress wave history curve.

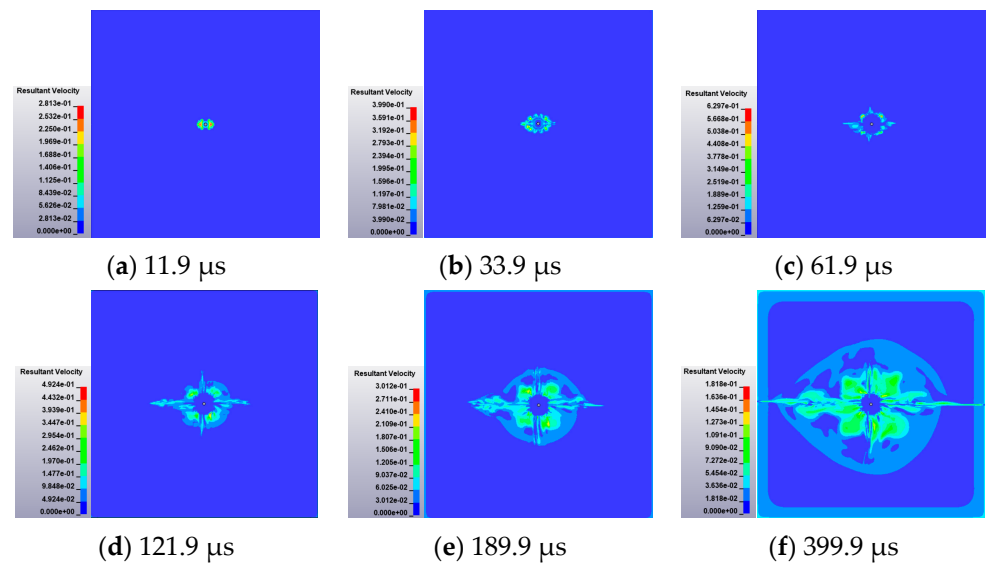


Figure 12. Variation process of detonation wave propagation velocity in the energy cumulative state.

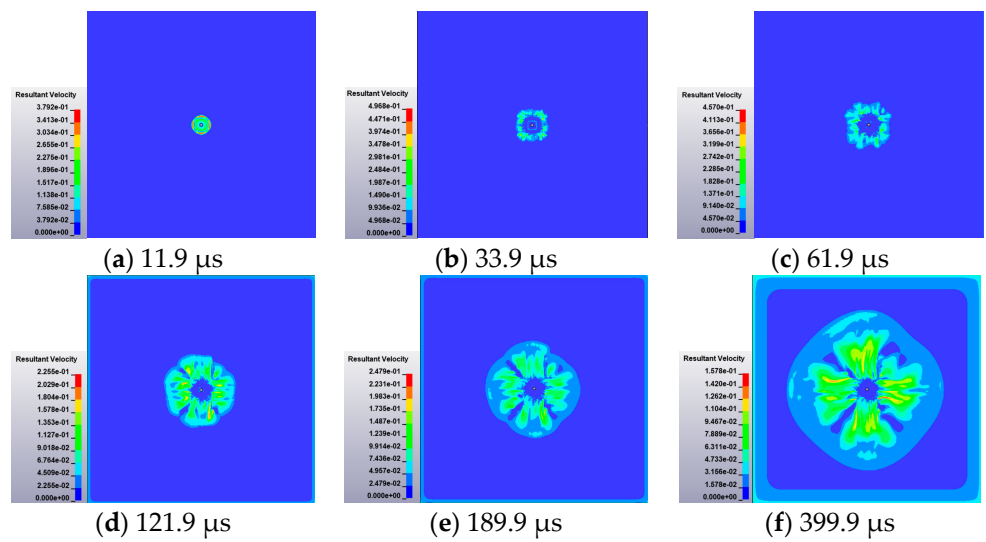


Figure 13. Variation process of detonation propagation velocity in the non-energy cumulative state.

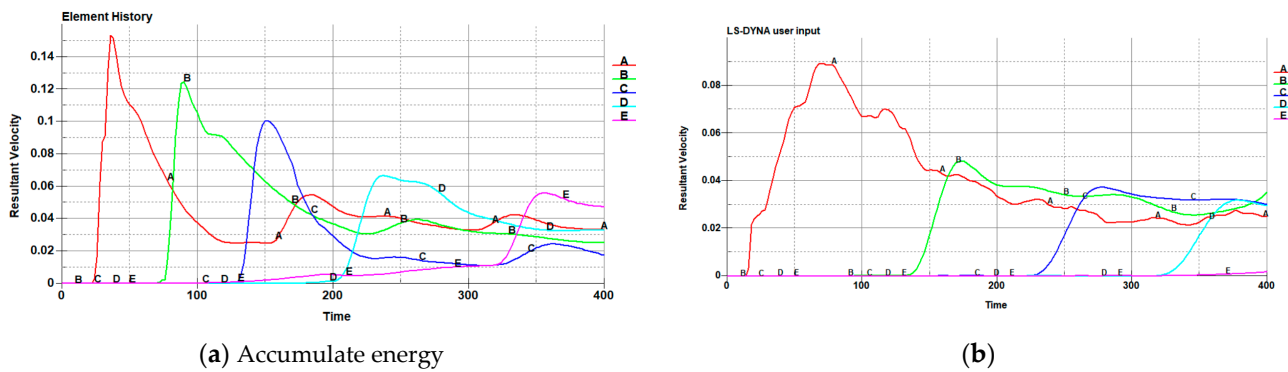


Figure 14. Detonation wave propagation velocity variation curve.

4.3.3. Rock Tension-Compression Stress and Rock Damage Evolution Process

It can be seen from rock tension and compression stress, rock damage cloud map, and history curve (Figures 15–20), in the energy cumulative state, at the beginning of blasting, that the detonation gas first ejects from the set direction, the stress concentration occurs in the set direction at 11.9 μs , and the stress wave propagates outward in a fan shape along the energy cumulative direction. Then, the detonation wave acts on the wall of the blasthole to form an initial crack, that is, the guiding crack, guides the fracture to continue to spread outward in this direction, and then, with the continued propagation of the stress wave, the damage area of the rock continues to expand. However, with the increase of time, the stress wave will continue to decrease, which will reduce the degree of rock damage, and at this time, the stress is mainly concentrated in the crack tip. Under the action of the “gas wedge”, the new crack at the tip is constantly under tension, and because the stress intensity factor at the tip is greater than the rock fracture toughness, the crack continues to expand. After 61.9 μs , the damage area is basically unchanged, and the stress of the surrounding rock of the blasthole decreases. Under quasi-static action of explosive gas, the crack expands under the tensile stress, forming a through crack. In ordinary blasting, due to the use of uncoupled charge. The detonation wave cannot act on the blasthole wall the first time. At 11.9 μs , the detonation wave is transmitted to the blasthole wall, and the tension and compression stress of the rock is mainly distributed around the blasthole. A high stress zone is formed on the rock around the blasthole, and the detonation wave stress strength greatly exceeds the tensile strength of the rock. At 33.9 μs , the rock around the blasthole is completely destroyed, the stress wave expands outward, and the damage range of the rock increases continuously. Moreover, under the action of the detonation wave, the rock around the blasthole continues to destroy, and because of the randomness of the detonation wave, irregular cracks are formed in the rock outside the blasthole. Between 33.9 μs and 121.9 μs , under the action of explosive stress wave, the failure range of rock increases continuously, and the maximum effective stress also increases. At 121.9 μs , the crack stops developing, the tension and compression stress of rock begins to attenuate, the effect on rock decreases until the explosive is exhausted, and the stress distribution of rock outside the blasthole becomes gradually uniform. Under the non-energy cumulative condition, the stress wave always propagates uniformly outward in a ring, and the effective stress at the same distance from the center of the hole is basically the same. Compared with the non-concentrated blasting, the cracks of the concentrated blasting are mainly distributed in the set direction of the concentrated tube, but not the cracks caused by the concentrated blasting spreading irregularly. Due to the existence of the energy cumulative tube, the stress factors are concentrated in the energy cumulative direction, which not only protects the integrity of the surrounding rock around the non-energy cumulative direction, but also can effectively precrack the roof and form an effective crack. Under the energy cumulative condition, the tension and compression stress of rock at each measuring point is about 2.3 times higher than that in the non-energy cumulative state. In both states, the tension-compression stress and rock damage decrease with the increase of the distance between the measuring point and the blasthole, but the interaction time between detonation wave and rock is longer in the energy cumulative state.

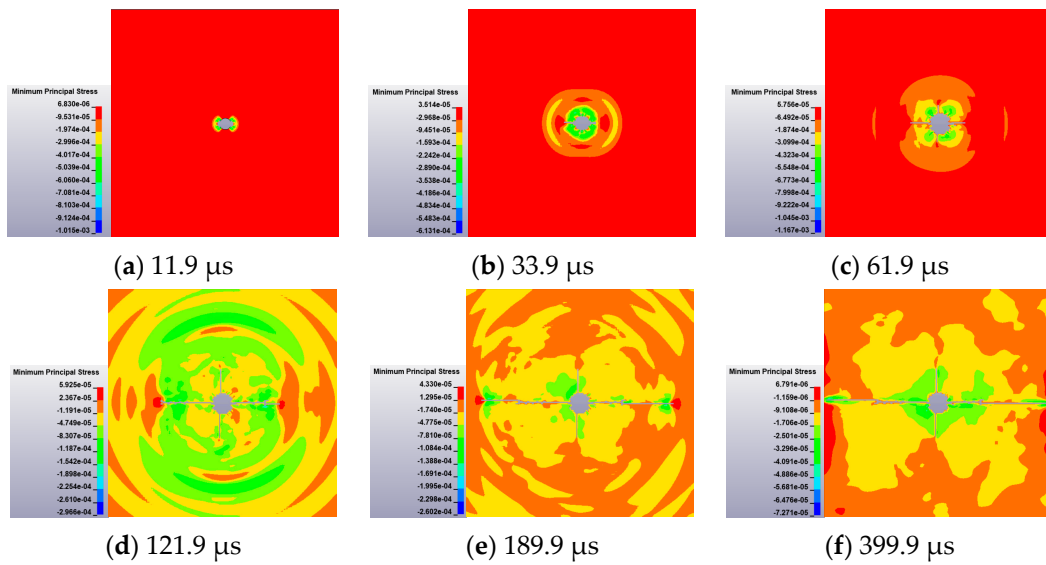


Figure 15. Variation process of tension and compression stress of rock under the energy cumulative condition.

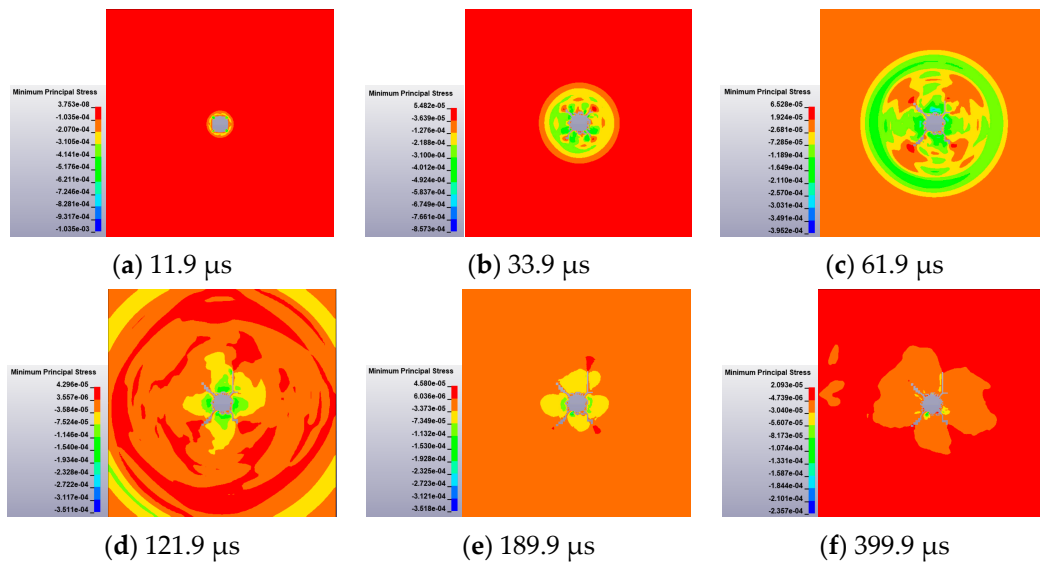


Figure 16. Variation process of tension and compression stress of rock under the non-energy cumulative condition.

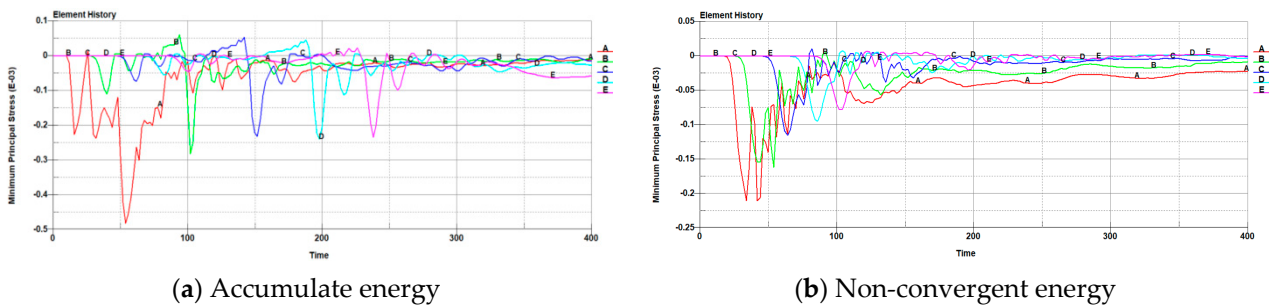


Figure 17. Stress variation curve of rock under tension and compression.

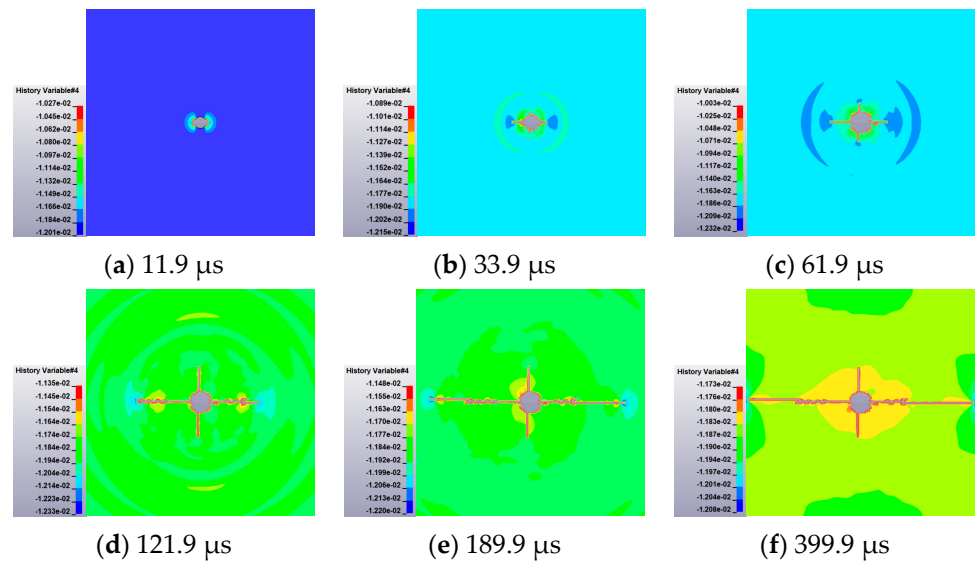


Figure 18. Damage evolution of rock under the energy cumulative condition.

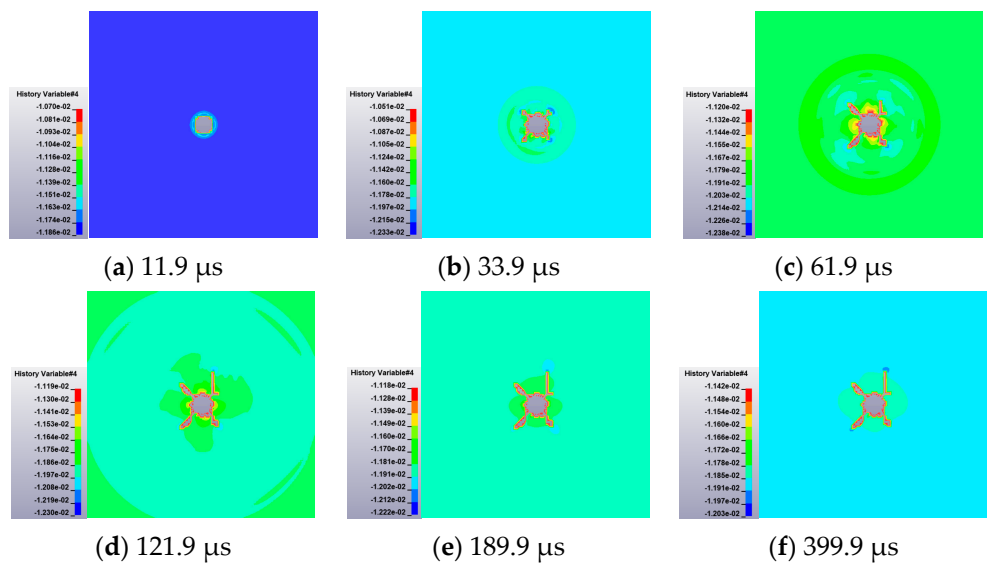


Figure 19. Damage evolution process of rock under the non-energy cumulative condition.

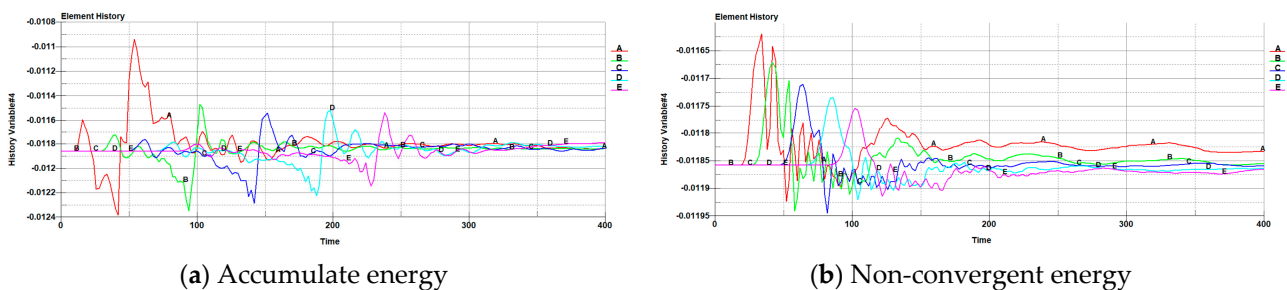


Figure 20. Damage history curve of rock.

4.3.4. Blasting Crack Displacement

It can be seen from Figure 4 that the cracks produced by non-concentrated blasting spread out uniformly with the blasthole at the center, resulting in irregular divergent cracks and the development of cracks are more uniform. It can be seen from Figures 3 and 21 that under the energy cumulative condition, the stress concentration occurs in the set direction

of the energy cumulative tube, and the detonation stress wave preferentially acts on the hole wall along the energy cumulative direction, resulting in an obvious guiding crack at 33.9 μs . Under the guidance of the guide crack, the subsequent cracks continue to extend in this direction until they run through, and there are fewer cracks in the non-energy cumulative direction. It can be seen from Figure 22 that the curve changes of each measuring point have an obvious dynamic load stage, static load stage, and stable stage. Under the energy cumulative condition, there are two kinds of action: the compressive strain and tensile strain, and the tensile strain is mainly affected by the compressive strain, while in the non-energy concentrated state, there is only the compressive strain. Under the energy cumulative condition, with the increase of distance, the peak value of the compressive stress at the five measuring points of Arecoire, C and D is gradually weakened, while the tensile stress is gradually increased, which is due to the concentrated tension in the set direction due to the action of the energy gathering device. The detonation pressure can be converted to the tensile effect on the surrounding rock in the set direction to the maximum extent, resulting in an effective slit surface. Compressive stress in the non-energy-gathering state decreases with the increase in the distance until it is 0. By comparison, it can be found that the detonation wave is enhanced in the energy cumulative direction by the energy cumulative device. With the formation of the guide crack, a large amount of detonation gas is poured in, which strengthens the load and lasts longer, resulting in effective slit cracks.

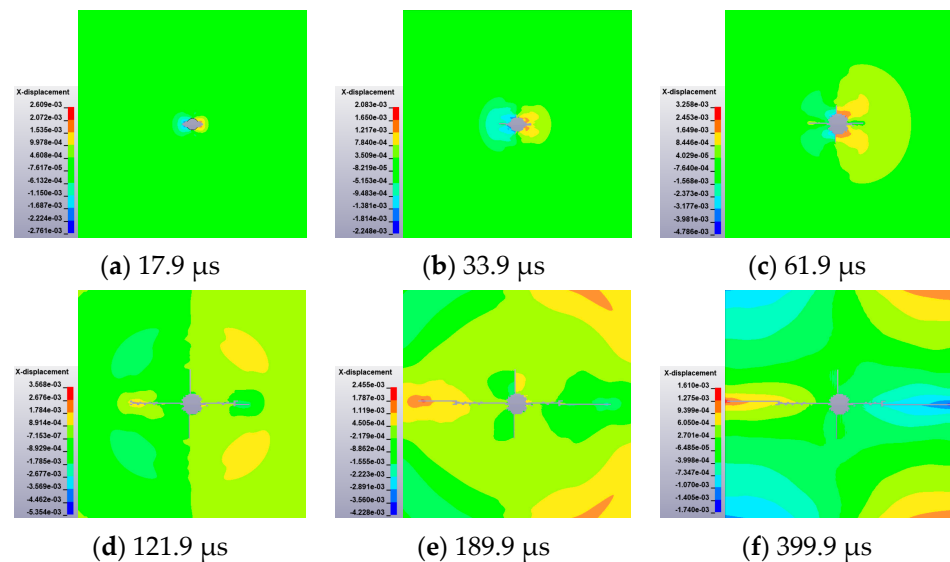


Figure 21. Evolution process of fracture displacement under the energy cumulative condition.

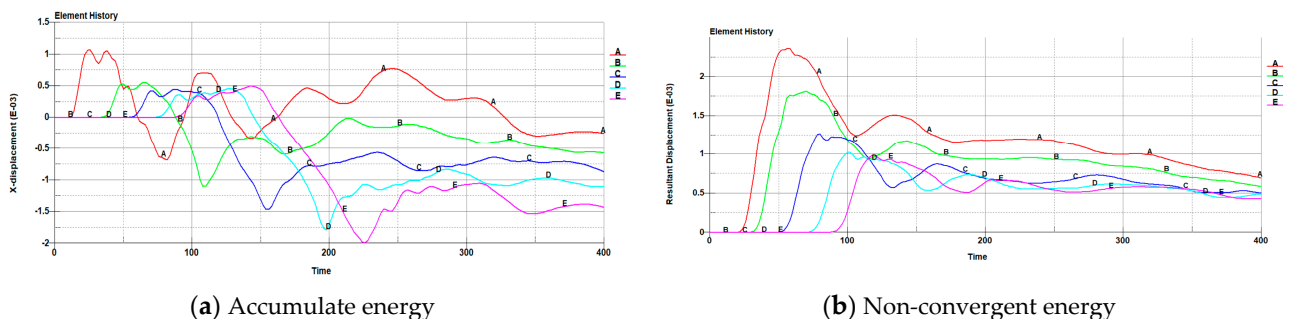


Figure 22. Fracture displacement evolution curve.

5. Field Test

5.1. Test Scheme

Experiments are carried out in the working face on the basis of numerical simulation, and the presplitting slit blasting materials is shown in Figure 23, including emulsion

explosives, gun mud, detonators, wires, energy accumulators, and connectors. In the field test, the diameter of the borehole is 50 mm, the optimum charge quantity in the stable area of the roof is 3:2, there are two concentrating tubes in each hole, the specification of the charge cartridge is $\phi 32 \times 200$ mm, and the quality is 300 g/roll. The optimum charge quantity in the compound broken roof area is 2:1, there are two energy collecting tubes in each hole, the specification of the charge cartridge is $\phi 32 \times 200$ mm, and the mass is 300 g/roll. The method of segmenting charge is adopted, and when the crack rate of this test reaches 80%, the charge structure is adopted in the follow-up test. When the crack rate is less than 80%, the charge needs to be increased. The slit hole is arranged at a certain angle between the side of the roadway and the roof, the angle between the crack hole and the plumb line is 15° , the hole depth is 5 m, and the sealing mud length is 2 m.

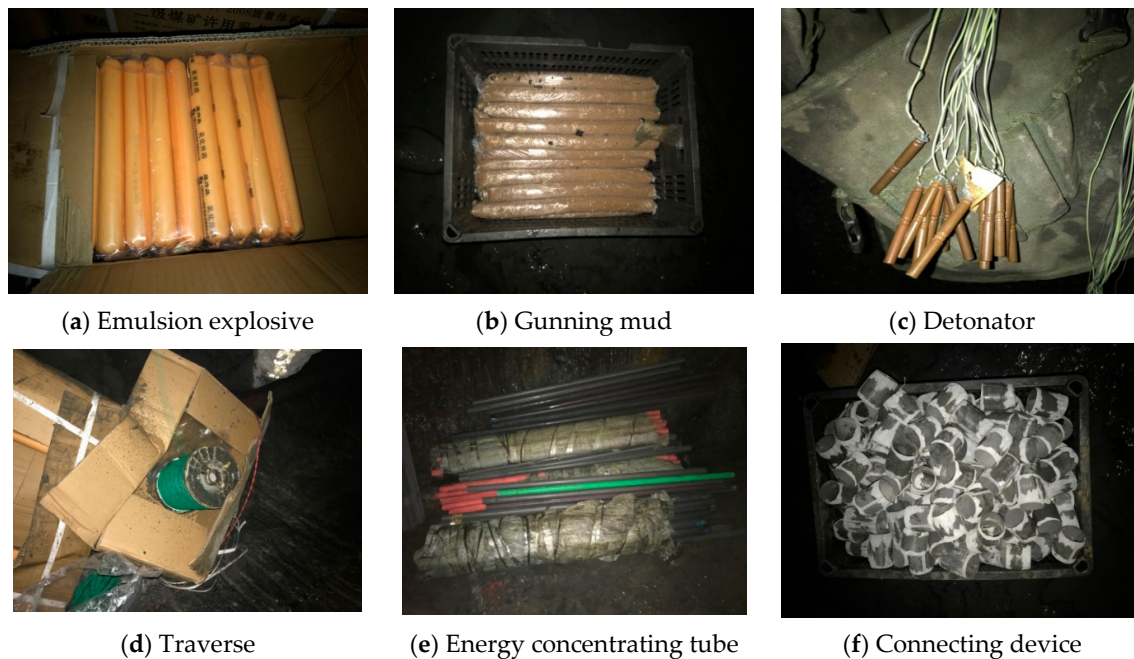


Figure 23. Presplitting slotting blasting material.

5.2. Test Process

First of all, DCA-45 roofs slotting hole drilling rig is used for drilling. The detonators and lead are installed in the roadway according to the blasting charge design parameters. Starting from the bottom of the hole, after the charge is finished, the lead is passed through the second energy concentrator, and the first energy concentrator is connected with the second one with connectors. Then, the charge is started and the leads are installed in the second tube, and so on, after which the charge of the concentrator is completed in turn. After all placements, the directional rod is used to adjust the slit direction of the energy concentrator, so that the slit direction of the energy concentrator is consistent with the cutting top line. Then, the hole is sealed with blasting mud, and finally, the blasting test is realized. The blasting process is shown in Figure 24.

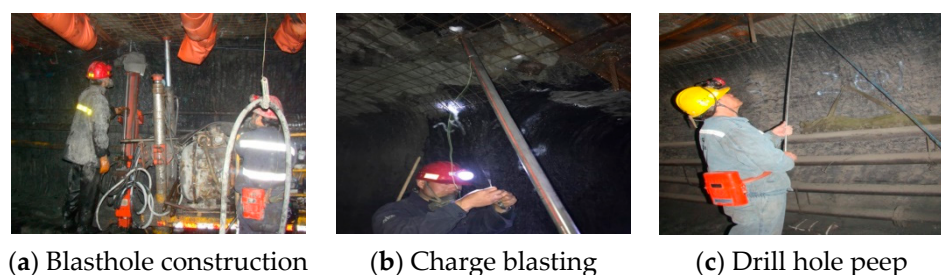


Figure 24. Construction process of energy cumulative blasting.

5.3. Analysis of Test Results

At the end of the test, a CXK6 snooping device was used to measure the length of the crack in the slit hole. The blasting results are shown in Figure 25. From the blasting results, it can be seen that under the action of energy cumulative blasting, there are two cracks on the inner hole wall and the outer rock wall of the blast hole, and the rock wall in the non-set direction still maintains good integrity. Therefore, the crack in the slit hole is a single crack surface, not multiple crack surfaces, and this kind of one-sided crack occurs in the shallow, middle, and deep parts of the hole. After the statistics, the average crack rate of the shaped blasting slit hole is 82%, which meets the requirement of the cracking rate. After presplitting, the roof collapse is shown in Figure 25c. Through the comparison of the results, it can be seen that the results of the field test and the numerical simulation are consistent, and the penetration cracks are produced in the energy cumulative direction. Therefore, directional energy-cumulative presplitting blasting can realize directional roof cutting.

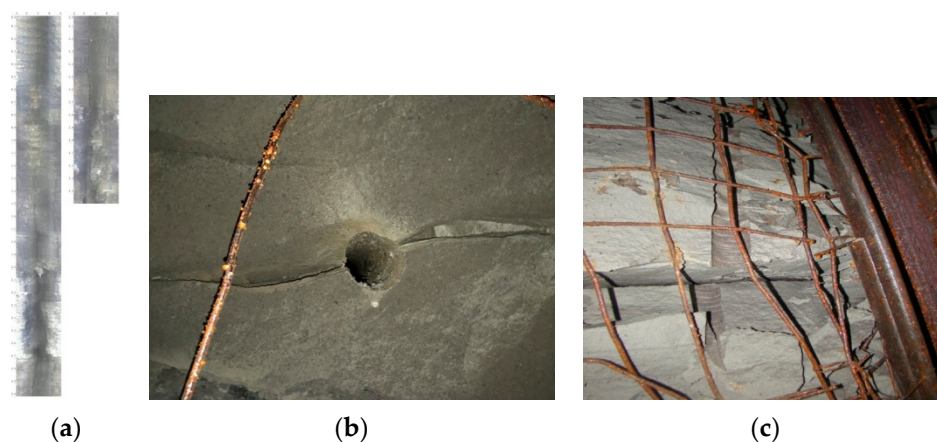


Figure 25. Blasting effect. (a) In-hole blasting effect. (b) Out-of-hole blasting effect. (c) Roof presplitting effect.

6. Conclusions

- (1) In the state of energy accumulation, the detonation wave produced by blasting gathered in the set direction, resulting in the concentration of tensile strain energy. Under the action of the energy accumulation device, the surrounding rock of the blasthole in the set direction was destroyed and an initial crack was formed. Under the action of the energy-accumulating jet, the crack continued to propagate until penetration. In the non-energy-gathering state, the detonation wave and energy produced by the explosion acted uniformly on the whole wall around the blast hole, resulting in divergent short cracks.
- (2) Under the action of detonation wave and detonation energy, two penetrating cracks in the set direction were formed in the surrounding rock under the condition of concentrated blasting, and the cracks developed irregularly around the blasthole under the non-concentrated blasting condition.
- (3) Through the field test of the 6302 working face in the Baoshan Coal Mine, two single cracks in the set direction were produced on the inner wall of the blast hole and the rock wall outside the hole, which met the cracking requirements. The field test results were consistent with the simulation results. Therefore, directional energy-concentrated presplitting blasting can cut off the connection between roadway roof and stope, effectively control roadway roof structure, and realize the effect of directional roof cutting.

Author Contributions: Conceptualization, E.W.; methodology, Z.S.; software, E.W. and Z.S.; validation, E.W.; formal analysis, Z.S.; investigation, E.W.; resources, E.W.; data curation, W.X.; writing—original draft preparation, E.W. and Z.S.; writing—review and editing, E.W.; visualization, J.F. and P.W.; supervision, E.W.; project administration, E.W.; funding acquisition, E.W. All authors have read and agreed to the published version of the manuscript.

Funding: This work was funded by the National Natural Science Foundation of China (Grant no. 52064042), the Inner Mongolia Natural Science Foundation (Grant no. 2020BS05004), and the Innovation Fund Project of Inner Mongolia University of Science and Technology (Grant no. 2019QDL-B34).

Institutional Review Board Statement: Not applicable.

Informed Consent Statement: Not applicable.

Data Availability Statement: All data included in this study are available upon reasonable request by contacting the corresponding author.

Acknowledgments: We are grateful to the anonymous reviewers for their insightful reviews on the manuscript, and to the editors for carefully editing the manuscript.

Conflicts of Interest: The authors declare no conflict of interest.

References

1. Dou, L.M.; He, X.Q.; Hu, H.E.; Jiang, H.E.; Jun, F.A.N. Spatial structure evolution of overlying strata and inducing mechanism of rock burst in coal mine. *Trans. Nonferrous Met. Soc. China* **2014**, *24*, 1255–1261. [[CrossRef](#)]
2. Gao, Y.; Wang, Y.; Yang, J.; Zhang, X.; He, M. Meso- and macro effects of roof split blasting on the stability of gate road surroundings in an innovative nonpillar mining method. *Tunn. Undergr. Space Technol. Inc. Trenchless Technol. Res.* **2019**, *90*, 99–118. [[CrossRef](#)]
3. Zhao, T.; Liu, C.; Yetilmezsoy, K.; Zhang, B.; Zhang, S. Fractural structure of thick hard roof stratum using long beam theory and numerical modeling. *Environ. Earth Sci.* **2017**, *76*, 751. [[CrossRef](#)]
4. Li, X.; Zhou, Z.; Lok, T.-S.; Hong, L.; Yin, T. Innovative testing technique of rock subjected to coupled static and dynamic loads. *Int. J. Rock Mech. Min. Sci.* **2007**, *45*, 739–748. [[CrossRef](#)]
5. He, M.; Cao, W.; Shan, R.; Wang, S. New blasting technology—Bilateral cumulative tensile explosion. *J. Rock Mech. Eng.* **2003**, *12*, 2047–2051. [[CrossRef](#)]
6. Singh, P.K.; Roy, M.P.; Paswan, R.K. Controlled blasting for long term stability of pit-walls. *Int. J. Rock Mech. Min. Sci.* **2014**, *70*, 388–399. [[CrossRef](#)]
7. Pan, Y.; Liu, Z. Study on multi-direction shaped charge blasting technology for coal seam containing hard dirt band with high gas and low permeability. *Sci. Technol. Prod. Saf. China* **2019**, *15*, 144–150. [[CrossRef](#)]
8. Ren, G. Study on Roof Cutting and Pressure Relief Technology of Gob Side Entry Retaining by Shaped Charge Blasting in Complex Thin Coal Seam. *Coal Technol.* **2022**, *41*, 17–22. [[CrossRef](#)]
9. Guo, F.; Zheng, X.; Wang, Z.; Wang, Y.; Xu, B.; Qi, J. Experimental Research on Roof-cutting Technology of Energy-gathered Blasting in Hongliulin Coal Mine. *Coal Technol.* **2022**, *41*, 51–54. [[CrossRef](#)]
10. Zong, Q.; Meng, D. Influence of different kinds of hole charging structure on explosion energy transmission. *J. Rock Mech. Eng.* **2003**, *4*, 641–645. [[CrossRef](#)]
11. Liang, H.; Guo, P.; Sun, D.; Ye, K.; Zou, B.; Yuan, Y. A study on crack propagation and stress wave propagation in different blasting modes of shaped energy blasting. *Vib. Shock* **2020**, *39*, 157–164+184. [[CrossRef](#)]
12. Guo, D.; Zhao, J.; Lu, P.; Zhai, M. Dynamic effects of deep-hole cumulative blasting in coal seam and its application. *J. Eng. Sci.* **2016**, *38*, 1681–1687. [[CrossRef](#)]
13. Yang, R.; Zuo, J.; Song, J.; Chen, S.; Xiao, C. Experimental study on the extension rule of crack group around a hole under explosive stress wave. *Vib. Shock* **2018**, *37*, 74–78. [[CrossRef](#)]
14. Esen, S.; Onederra, I.; Bilgin, H.A. Modelling the size of the crushed zone around a blasthole. *Int. J. Rock Mech. Min. Sci.* **2003**, *40*, 485–495. [[CrossRef](#)]
15. Shi, Q.; Zheng, H.; Wang, Y.; Yun, M.; Wu, S.; Li, T.; Zhang, H. Study on parameters of blast hole spacing for gob side entry retaining by bidirectional shaped charge blasting. *Coal Mine Saf.* **2022**, *53*, 219–225. [[CrossRef](#)]
16. Wu, B.; Wei, H.; Xu, S.; Nong, Z.; Huang, J. Research on Numerical Optimization of Smooth Blasting Layer Parameters of Shaped Energy Smooth Blasting. *Non-Ferr. Met. Eng.* **2020**, *10*, 113–121. [[CrossRef](#)]
17. Song, J.; Kim, K. Micromechanical modeling of the dynamic fracture process during rock blasting. *Int. J. Rock Mech. Min. Sci. Geomech. Abstr.* **1995**, *33*, 387, 393–391, 394. [[CrossRef](#)]
18. Cho, S.H.; Kaneko, K. Influence of the applied pressure waveform on the dynamic fracture processes in rock. *Int. J. Rock Mech. Min. Sci.* **2004**, *41*, 771–784. [[CrossRef](#)]

19. Xia, B.; Liu, C.; Lu, Y.; Liu, Y.; Ge, Z.; Tang, J. Experimental study of propagation of directional fracture with slotting hydraulic blasting. *J. Coal* **2016**, *432*, 438. [[CrossRef](#)]
20. Zhang, Z. On the Initiating, Growing Branching and Sloping of Crack in Rock Blasting. *Blasting* **1999**, *16*, 21–24.
21. Zong, Q. Investigations into mechanism of crack formation for grooved hole-well blasting. *J. Geotech. Eng.* **1998**, *20*, 30–33. [[CrossRef](#)]
22. Zhang, Q.; Zhang, R. Numerical Simulation of Explosion Using ALE Method. *Mech. Q.* **2005**, *4*, 639–642. [[CrossRef](#)]
23. He, M.; Zhang, X.; Zhao, S. Directional Destress with Tension Blasting in Coal Mines. *Procedia Eng.* **2017**, *191*, 89–97. [[CrossRef](#)]
24. Zhang, S.; Zhang, C.; Wang, Y.; Wang, C. Directional Fracture Blasting in Open-off Cut of Fully-Mechanized Caving Mining Face During Primary Mining. *J. Beijing Inst. Technol.* **2017**, *37*, 135–140. [[CrossRef](#)]
25. Zhang, X.; Zhang, C.; Zeng, J. Numerical Simulation of Reasonable Radius of Empty Holes on Both Sides of Shaped Structure Based on ANSYS/LS-DYNA. *Coal Technol.* **2019**, *38*, 118–120. [[CrossRef](#)]
26. Zhao, Z.; Ouyang, F.; He, F.; Xu, X.; Yang, Y.; Xu, R. Study on key parameters of bidirectional shaped charge blasting for gob side entry retaining with roof cutting and pressure relief. *Coal Mine Saf.* **2022**, *53*, 226–233. [[CrossRef](#)]